



**HAL**  
open science

# Ray Optics Analysis Explanation of Beam-Splitting Condition in Fabry-Pérot Antennas

Etienne Perret, Raul Guzman Quiros

► **To cite this version:**

Etienne Perret, Raul Guzman Quiros. Ray Optics Analysis Explanation of Beam-Splitting Condition in Fabry-Pérot Antennas. IEEE Access, 2018, 6, pp.32360-32366. hal-02054101

**HAL Id: hal-02054101**

**<https://hal.science/hal-02054101>**

Submitted on 1 Jul 2020

**HAL** is a multi-disciplinary open access archive for the deposit and dissemination of scientific research documents, whether they are published or not. The documents may come from teaching and research institutions in France or abroad, or from public or private research centers.

L'archive ouverte pluridisciplinaire **HAL**, est destinée au dépôt et à la diffusion de documents scientifiques de niveau recherche, publiés ou non, émanant des établissements d'enseignement et de recherche français ou étrangers, des laboratoires publics ou privés.

# Ray Optics Analysis Explanation of Beam-Splitting Condition in Fabry-Pérot Antennas

Etienne Perret, *Senior Member, IEEE*, Raúl Guzmán-Quirós

**Abstract**—This paper presents a theoretical analysis where general and accurate formulas for the design of Fabry-Pérot antennas (FPA) are derived from a simple ray optics approach. The beam-splitting condition predicted from the leaky-wave (LW) theory is analyzed here from ray optics analysis. Excellent agreement is observed with the results obtained from the LW analysis in a significant frequency range. Thereby, these expressions allow to design FPAs accurately without performing dispersion analysis of the leaky modes inside the structure.

**Index Terms**— Fabry-Pérot resonant cavity antennas, leaky wave antenna, ray optics analysis, splitting condition.

## I. INTRODUCTION

FABRY-PÉROT antennas (FPA) introduced by Trentini [1] have been of high interest because of its high directivity and structural simplicity. Based on the use of a partially reflecting surface (PRS), as shown in Fig. 1a, its radiation mechanism has given rise to several works based on analytical developments focused on it [2]-[7]. Firstly, a simple ray optics analysis was employed to model their response [1], [3], taking into account the presence of multiple reflections between the ground plane and the PRS (see Fig. 1a). It has been observed that this approach is accurate enough as a first step design of these antennas [3]. A useful expression describing the relation between the PRS reflection coefficient  $R = re^{j\varphi}$  (where  $r$  is the magnitude and  $\varphi$  the phase), the height of the PRS ( $h$ ) over the ground plane, the operating frequency  $f$  and the power pattern  $P_T$  function of the observation angle  $\theta$  has been derived in [1, eq. (3)]:

$$P_T(\theta) = \frac{1 - r(\theta)^2}{1 + r(\theta)^2 - 2r(\theta) \times \cos\left(\varphi(\theta) - \pi - \frac{4\pi h}{\lambda_0} \cos(\theta)\right)} F^2(\theta) \quad (1)$$

where  $\lambda_0 = 2\pi/k_0$ , the wavelength in free space and  $F^2(\theta)$  is the radiation pattern of the primary antenna, that could equal 1 if this primary feed is assumed isotropic. This analytical formula is obtained assuming an infinite PRS and ground plane.

Etienne Perret is with the University of Grenoble Alpes, Grenoble INP, LCIS, 50 rue Barthélémy de Laffemas - BP 54, 26902, Valence Cedex 9 - France. He is also with the Institut Universitaire de France (IUF). (e-mail: etienne.perret@lcis.grenoble-inp.fr). Raul Guzman Quiros was with the University of Grenoble Alpes, Grenoble INP, LCIS. Currently, he is not affiliated to any institution. (e-mail: raul.guzman.quirós@gmail.com).

From (1), it is obvious that the maximum power at broadside ( $\theta = 0$ ) is obtained when the resonance condition is satisfied:

$$\varphi(0) = \frac{4\pi h}{c} f - (2N - 1)\pi, \quad N = 0, 1, 2 \dots \quad (2)$$

In practice, (2) is used to do a first design of the FPA. Then in a second step, a full wave simulation can be used to optimize the real prototype with a finite antenna length and real excitation.

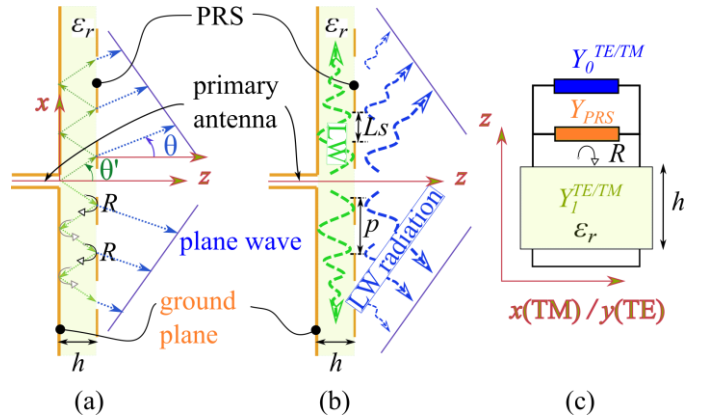


Fig. 1. Schematic diagram of the FPA and geometry of the PRS. (a) LWA and illustration of the simple ray analysis of the resonant cavity antenna formed by a PRS over a ground plane, (b) illustration of the LWA approach, (c) TEN model and equation.

A few decades later, the leaky-wave theoretical principle was applied to describe the fundamental operation of FPAs [8], [5] (see Fig. 1b). This model allows to predict the radiation characteristics by predicting the propagation of radiative transverse electric (TE) and/or transverse magnetic (TM) leaky modes (LM) inside the Fabry-Pérot cavity (FPC) (see the illustration depicted in Fig. 1c). To determine the complex propagation constants of these LMs, a transverse equivalent network (TEN) can be engineered and transcendental resonance equation must be solved by numerical methods. The wavenumbers of these modes are useful data to obtain the radiation response of such antenna. Moreover, the far field radiated by the FPA can be computed from these propagation constants [3]. Based on this physical interpretation, lots of analytical expressions can be derived to help designers [7].

From this theory, the maximization of the power density radiated at broadside of such antenna (see Fig. 1a) can be derived analytically [4, eq. (4)], and the optimum condition

also known as the beam-splitting condition corresponds to the equation  $\alpha=\beta$  [4]. Simple equations [4, eq. (20), (21)] can be obtained respectively to choose the cavity height  $h$  and the corresponding leaky-wave (LW) phase  $\beta$  and attenuation constants  $\alpha$  for a given frequency and PRS.

In this paper, the approach introduced in 4 to derive the splitting condition is applied for the first time on the power pattern formula (1) obtained from the ray optics analysis. The splitting condition and several formulas useful for antenna design are then derived. Contrary to the equations derived from the LW analysis and expressed in terms of the propagation constants, these formulas are functions of the magnitude  $r$  and the phase of the reflection coefficient of the PRS  $\varphi$ . The accuracy and the validity range of these formulas are evaluated and compared with the ones obtained from a LW analysis.

## II. RAY OPTICS ANALYSIS – THE SPLITTING CONDITION

From the ray optics approach, an analytic formula for the power pattern of the LWA shown in Fig. 1a is obtained by doing the summation of the transmitted rays:

$$P_T(\theta, f, \epsilon_r) = \frac{1 - r^2}{1 + r^2 - 2r \times \cos(\varphi - \pi - 2\sqrt{\epsilon_r}k_0 h \cos(\theta'))} \quad (3)$$

Contrary to previous works such as [1]-[3], the presence of a dielectric substrate of permittivity  $\epsilon_r$  between the PRS and the conductive plane is considered in this work. Both amplitude  $r$  and phase  $\varphi$  of the PRS reflection coefficient are a function of the angle of incidence  $\theta'$  corresponding to the ray propagating inside the cavity filled with a dielectric substrate of relative permittivity  $\epsilon_r$  and thickness (cavity height)  $h$ . The radiation angle  $\theta$  in free space is linked to  $\theta'$  by the Snell–Descartes law:

$$\theta' = \text{asin}\left(\frac{1}{\sqrt{\epsilon_r}} \sin(\theta)\right) \quad (4)$$

The PRS reflection coefficient ( $R$  in Fig. 1c) can be linked to the phase  $\beta$  and the attenuation constants  $\alpha$  by using the equivalent circuit of the transverse section of the structure shown in Fig. 1c [3]. Note also that the TEN introduces the PRS as an admittance  $Y_{PRS}=j\bar{B}/\eta_0$ , where  $\eta_0$  is the free-space characteristic impedance and  $\bar{B}$  the normalized susceptance. For the sake of clarity, a one-dimensional antenna is under consideration, so only the TE mode is considered in this study. Therefore, the admittances for the TE polarization have the following known expressions [4]:

$$Y_0 = \frac{|\cos\theta'|}{\eta_0}, Y_1 = \frac{\sqrt{\epsilon_r}|\cos\theta'|}{\eta_0} \quad (5)$$

where  $Y_0$  is the free space characteristic admittance and  $Y_1$  the characteristic admittance of the substrate medium inside the FPC (see Fig. 1c). Then, the reflection coefficient  $R$  is obtained easily from microwave transmission line theory:

$$R(\theta, \epsilon_r) = [1/(Y_{PRS} + Y_0) - 1/Y_1] / [1/(Y_{PRS} + Y_0) + 1/Y_1]$$

For  $\theta = 0$ , an analytical expression of  $r$  and  $\varphi$ , function of  $\bar{B}$  can be easily derived:

$$r(0, \epsilon_r) = \frac{\left(\left((\sqrt{\epsilon_r} + 1)(\sqrt{\epsilon_r} - 1) - \bar{B}^2\right)^2 + 4\epsilon_r \bar{B}^2\right)^{1/2}}{(\sqrt{\epsilon_r} + 1)^2 + \bar{B}^2}$$

$$\tan(\varphi(0, \epsilon_r)) = \frac{-2\bar{B}\sqrt{\epsilon_r}}{(\sqrt{\epsilon_r} + 1)(\sqrt{\epsilon_r} - 1) - \bar{B}^2} \quad (6)$$

To establish the splitting condition, the same approach as the one introduced in [4] is done afterwards. For the sake of simplicity, let us consider the structure where the PRS is separated from the ground plane by a vacuum layer ( $\epsilon_r = 1, \theta = \theta'$ ). The derivative of the denominator  $DP_T$  in (3) with respect to the angle of incidence  $\theta$  is:

$$DP_T(\theta)' = 2r \times r' - (2r' \times \cos(\Phi) - r \times \sin(\Phi) \times \varphi') \quad (7)$$

where  $\Phi = \varphi - \pi - 2k_0 \times h \times \cos(\theta)$ . The stationary point of  $P_T$  can be found by equating (7) to zero. From (7), at  $\theta = 0$ , the maximum of  $P_T$  is obtained when  $\Phi = \varphi - \pi - 2k_0 \times h = 2N\pi, N = 0, 1, 2 \dots$  which exactly corresponds to (2). A second condition is assumed on  $r$ , which is the variation of the reflection magnitude with the angle of incidence does not varies significantly when  $\theta$  goes to zero ( $r'(\theta) \approx 0$ ). This second condition is not restrictive in practice for this kind of antenna, as the variation of  $r$  when  $\theta$  is small, can be considered close to zero. Concerning the condition on  $\Phi$ , this result means that the classical expression (2) is met theoretically when the splitting condition  $\alpha=\beta$  obtained by the LW approach is satisfied. In such case, a single maximum at broadside ( $\theta = 0^\circ$ ) is observable on the radiation power pattern.

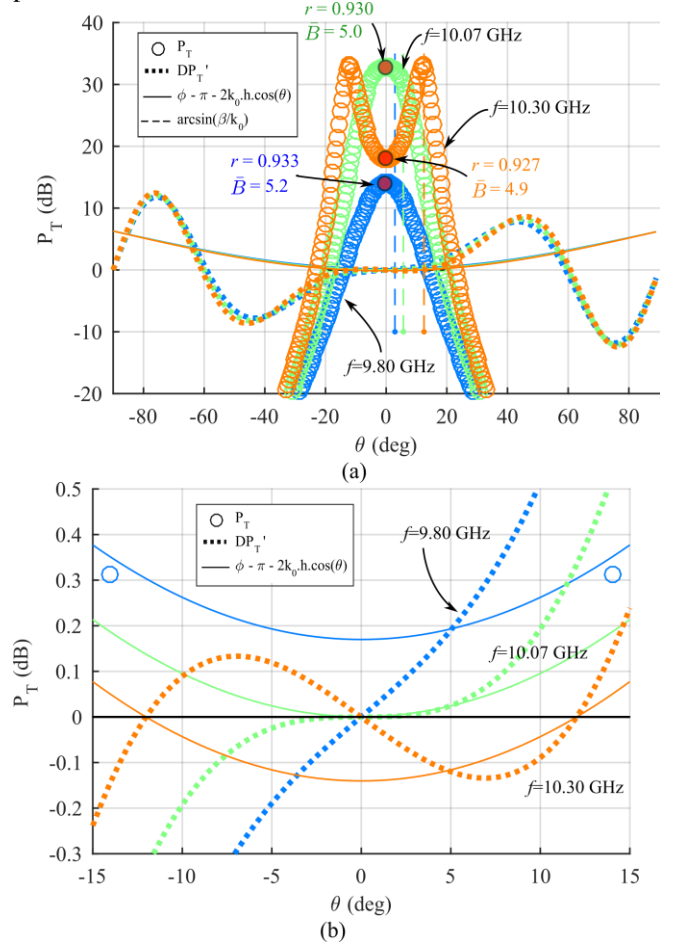


Fig. 2. (a) Radiated power density vs  $\theta$  for 3 frequencies around the splitting condition  $f=10.07$  GHz. (b) Zoom on the neighbourhood around  $\theta=0^\circ$ . The FPA is shown in Fig. 1:  $p=5$ mm,  $L_s=4$ mm,  $\epsilon_r=1$ ,  $h=14$  mm. The corresponding coefficients  $\bar{B}$  and  $r(0,1)$  are given at broadside in Fig. 2a.

This can be observed in Fig. 2, where the variation of the radiated power density (3) with the angle of incidence  $\theta$  for three frequencies in the neighborhood of the splitting condition frequency are shown in Fig. 2. The first derivative of  $DP_T$ , and the expression  $\Phi$  are also plotted. A LWA with a metallic slot-based frequency selective surface (FSS) has been considered (see Fig. 1). At the splitting frequency ( $f_{sc}=10.07\text{GHz}$ ), and assuming  $r'(\theta_{sc}) \approx 0$ , it can be observed that  $P_T$  is maximum at  $\theta = 0$ , where  $\Phi$  is also equal to zero (so resonance equation is met) (see Fig. 2b). For a higher frequency, the splitting condition is not met, so two symmetric main radiation lobes pointing at  $(\theta_{sc}, -\theta_{sc})$  are expected. This is observed if a frequency slightly higher than  $f_{sc}$  is analyzed, e.g.  $f=10.30\text{GHz}$  (see Fig. 2). In this case, the expression  $\varphi - \pi - 2k_0 \times h \times \cos(\theta) = 2N\pi$  is met at  $(12^\circ, -12^\circ)$ , matching the angles where  $P_T$  is maximum. Finally, it is also worth to note that for  $f=9.80\text{GHz}$ , which is lower than  $f_{sc}$ ,  $DP_T(\theta)' = 0$  at  $\theta = 0$ , but  $\Phi = 0$  is not met for any  $\theta$ , so the FPA is not resonating and power at broadside is not optimal (the antenna is operating inside the cutoff region of the FPC).

#### a) Optimization condition for the FPC height

Equation (2) can be used to compute the cavity height  $h$ , filled with a dielectric substrate  $\epsilon_r$ , and respecting the splitting condition at the desired frequency  $f$ , for  $\theta = \theta' = 0$ :

$$h = \frac{\varphi(0) - (2N - 1)\pi}{2\sqrt{\epsilon_r}k_0} = \frac{\text{atan}\left(\frac{-2\bar{B}\sqrt{\epsilon_r}}{(\sqrt{\epsilon_r} + 1)(\sqrt{\epsilon_r} - 1) - \bar{B}^2}\right) - (2N - 1)\pi}{2\sqrt{\epsilon_r}k_0} \quad (8)$$

Equation [4, eq. (20)], is an optimization condition for  $h$  that has also been derived from the dispersion equation (LW theory). Note that the following approximations have been taken into account to obtain [4, eq. (20)]:  $\alpha=\beta < 0.5$  and  $\bar{B} > 3$ . Expressions [4, eq. (20)] and (8) are both plotted in Fig. 3 for different values of  $\epsilon_r$ . For each value of  $\bar{B}$  and by considering the splitting condition  $\alpha=\beta$ , the substrate thickness  $h$  and  $\alpha$  have also been computed by solving the Transverse Resonance Equation (TRE) derived from the TEN:

$$Y_0 + Y_{PRS} = jY_1 \cot\left(h\sqrt{\epsilon_r k_0^2 - [\beta - j\alpha]^2}\right) \quad (9)$$

Both approximations from the ray optics and the LWA analysis are seen to be very accurate when  $\bar{B} \geq 3$ . For lower values of  $\bar{B}$ , (8) can be modified [noted in Fig. 3 as (8) mod] by adding the term  $-(1 + \bar{B})/\bar{B}^2 + \epsilon_r^{1/4}$  in the argument of the arctangent function in (8), in order to increase its range of validity. Indeed, a better accuracy is now also obtained for lower values of  $\bar{B} < 3$  when this modification is introduced, as observed in Fig. 3.

#### b) Formula of the LM phase and attenuation constants

An approximated expression for the LM wavenumber was also introduced in [4]. Equation [4, eq. (21)], can be used when the splitting condition is met for the antenna, but only when  $\alpha=\beta \ll 1$  and for large  $\bar{B}$ . Based on the ray analysis, it is also possible to derive an accurate expression. This formula of the LM wavenumber can be found by equating (3) to [4, eq. (4)], which corresponds here to (10):

$$P_{T[4]} = \frac{|E_0|^2(\beta^2 + \alpha^2)\cos^2(\theta)}{(k_0^2 \sin^2\theta - \beta^2 + \alpha^2) + 4 + \alpha^2\beta^2} \quad (10)$$

where the electric field amplitude  $E_0$  is similar to  $F(\theta)$  previously introduced in (1). Indeed, both equations correspond to the radiated power density by the antenna, respectively derived from the ray analysis and the LWA approach respectively. As proved in Appendix I, when we consider the splitting condition  $\alpha=\beta$  at  $f_{sc}$ , and (2) at broadside  $\theta = \theta' = 0$ , the following formula can be derived:

$$\alpha = \beta = \frac{\sqrt{\epsilon_r}k_0[1 - r(0, \epsilon_r)]}{\sqrt{\pi[1 - r(0, \epsilon_r)^2]}} \quad (11)$$

The frequency chosen to compute (11) can be noted as the splitting frequency  $f_{sc}$ . For the lossless structure under study, a comparison between (11), [4, eq. (21)] and the value extracted from the TEN model is given in Fig. 4. Contrary to the asymptotic expression [4, eq. (21)], (11) shows very good agreement in the full range of  $\bar{B}$ .

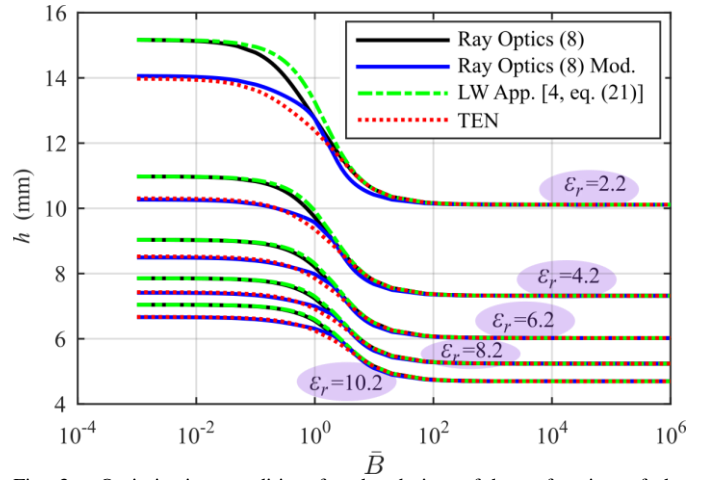


Fig. 3. Optimization condition for the design of  $h$  as function of the normalized shunt susceptance  $\bar{B}$ . Comparison between (8) obtained from the ray analysis and  $h = 1/(k_0\sqrt{\epsilon_r}) \times [\text{acot}(\bar{B}/\sqrt{\epsilon_r}) + \pi]$  obtained from the dispersion equation [4, eq. (20)] (LWA - Approximation), and from the full TEN resolution (LWA). A modified expression, (8) mod, is also shown for comparison. The structure is shown in Fig. 1a.  $\epsilon_r = 2.2$ ,  $f = 10\text{GHz}$ .

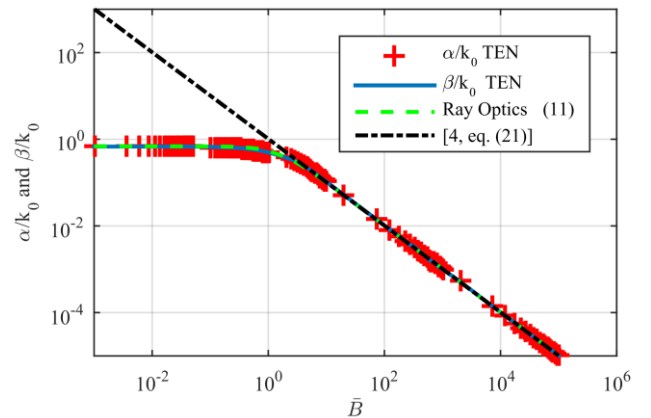


Fig. 4. Normalized attenuation  $\alpha/k_0$  and phase  $\beta/k_0$  constants of the TE LM versus the normalized shunt susceptance  $\bar{B}$ . The corresponding antenna is plotted in Fig. 1. Expression (8) mod has been used to compute the cavity height  $h$  for each value of  $\bar{B}$  in the case of the TEN computation.  $\epsilon_r = 2.2$ ,  $f_{sc} = 10\text{GHz}$ .

### III. GENERAL FORMULA OF THE RADIATIVE POWER

In a neighborhood of the frequency at which the splitting condition is met, it is now possible to extend the accuracy of the formula of the radiative power (3). The objective is to obtain exactly the same results between this formula expressed as functions of  $\theta, f, \epsilon_r, \bar{B}$  and the ones from the expressions derived with the LWA theory (expressed with  $\alpha, \beta$ ), thus obtaining an accurate and direct analytical expression which do not need solving the TEN to obtain the LM wavenumber.

Equation [2, eq. 13], which has been firstly introduced, gives the radiated power density. It is easy to observe that this equation corresponds to (10) multiplied by the coefficient  $1/(\beta^2 + \alpha^2)$ . Using the previous work done to derive (11), as proved in Appendix II, the following expression can be derived:

$$P_{\text{ray}}^{\text{C}}(\theta, f) = P_{\text{T}}(\theta, f, \epsilon_r) \frac{\pi^2}{(2\epsilon_r k_0^2)^2} \frac{1 - r(0, \epsilon_r)^2}{[1 - r(0, \epsilon_r)]^2} \cos(\theta) \quad (12)$$

As mentioned,  $r$  and  $\varphi$  can always be rewritten in terms of  $\bar{B}$  [e.g.  $r(0, \epsilon_r)$  is given by (6)]. The comparison between  $P_{\text{ray}}^{\text{C}}$  and [2, eq. 13] is plotted in Fig. 5. A very good agreement can be seen. A parametric study has shown that this agreement is obtained whatever  $\epsilon_r$  and  $f$ , but for  $\bar{B} \geq 1$ . For smaller values of  $\bar{B}$ , good accuracy is obtained only when  $f = f_{\text{sc}}$ . Strictly speaking, this corresponds to the frequency for which (12) has been analytically derived (see Appendix II).

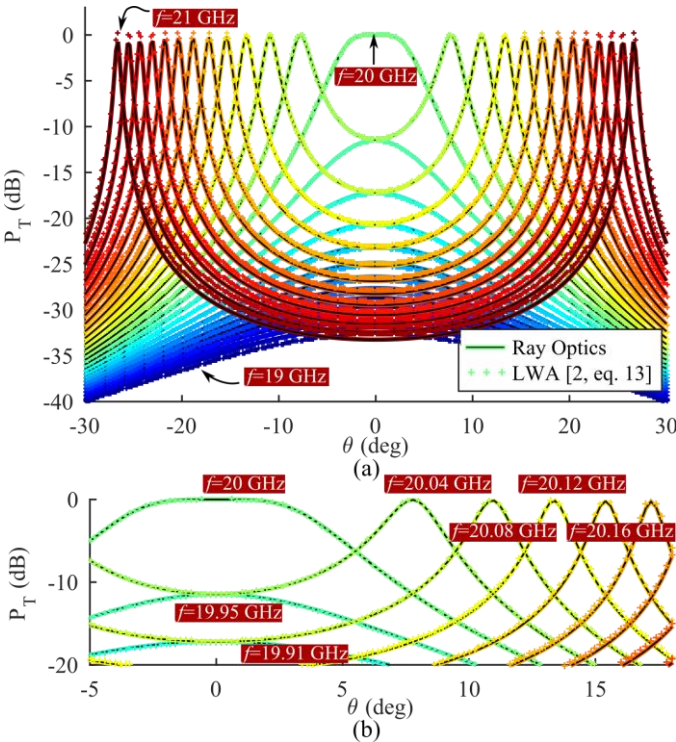


Fig. 5. a) Radiative power density as a function of  $\theta$  in the neighbourhood of the splitting frequency ( $f_{\text{sc}}=20\text{GHz}$ , frequency range: 19 GHz – 21 GHz). Comparison between (12) (ray analysis) and [2, eq. 13] (LWA approach).  $\bar{B} = 20$ ,  $\epsilon_r=2.2$ ,  $h=5.2\text{mm}$ . (b) Zoom on Fig. 5(a) on a smaller range of  $\theta$ . All curves are normalized to the value derived for  $f_{\text{sc}}=20\text{GHz}$ ,  $\theta = 0$ .

The same approach has been done with (10), which is a more accurate formula. Indeed, the presence of the coefficient  $(\beta^2 + \alpha^2)$  allows to take into account the variation of the radiated power magnitude when the beam pointing is off broadside. The following formula has been obtained:

$$P_{\text{ray}}^{\text{L}}(\theta, f) = P_{\text{T}}(\theta, f, \epsilon_r) \frac{\pi}{2\epsilon_r k_0^2} g(f) \cos(\theta) \quad (13a)$$

with

$$g(f) = \left\{ 1 + \left[ \frac{4\bar{B}^2}{\epsilon_r^{1/2} f_{\text{sc}}} (f_{\text{sc}} - f) \right]^{2.11} \right\}^{1/2}$$

Note that when  $f = f_{\text{sc}}$ ,  $P_{\text{ray}}^{\text{L}}$  is simple equal to:

$$\begin{aligned} P_{\text{ray}}^{\text{L}}(\theta, f_{\text{sc}}) &= P_{\text{T}[4]}(\theta, f_{\text{sc}}) = 2\alpha^2 \cdot P_{\text{ray}}^{\text{C}}(\theta, f_{\text{sc}}) \\ &= P_{\text{T}}(\theta, f_{\text{sc}}, \epsilon_r) \frac{\pi}{2\epsilon_r k_0^2} \cos(\theta). \end{aligned} \quad (13b)$$

Equation (13b), which is valid for  $f = f_{\text{sc}}$ , can be derived analytically with the use of (17) and (21) given in Appendix I and by multiplying the results by  $\cos(\theta)$  to consider the angle dependency. Expression (13a) has been obtained from (13b) with a curve fitting approach. Fig. 6 shows the comparison between the two formulas. Again a very good agreement is obtained, especially for (13b) where both curves are superimposed perfectly whatever  $\epsilon_r$  and  $f_{\text{sc}}$ . Contrary to the results plotted in Fig. 5, in Fig. 6, the magnitude of the peak apex are not constant which is linked to the presence of the term  $(\beta^2 + \alpha^2)$ . The validity range of (13) is comparable with the one of (12). A comparison study between (13) and (10) is given in Fig. 7 by varying  $\bar{B}$  and  $f$  on a wide range. Fig. 7a presents the absolute error for the same antenna already used in Fig. 6. In Fig. 7b the radiative power density as a function of  $\theta$  for 4 specific couples of values ( $\bar{B}$ ,  $f$ ) is given. The absolute error for the same structure but with  $\epsilon_r = 10$  is also given in Fig. 7c. A good agreement is obtained on a wide range of  $\bar{B}$  and  $f$  values. This is especially true for  $f = f_{\text{sc}}$ , where the data comparison shows a very good accordance between both expressions: (13b) and (10). This result validates the accuracy of (11).

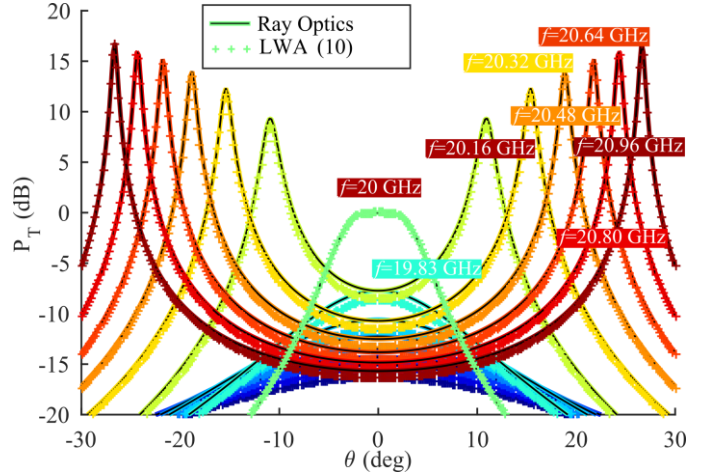


Fig. 6. Radiative power density as a function of  $\theta$  in the neighbourhood of the splitting frequency ( $f_{\text{sc}}=20\text{GHz}$ , frequency range: 19 GHz – 21 GHz). Comparison between (13) (ray analysis) and (10) (LWA approach).  $\bar{B} = 20$ ,  $f_{\text{sc}}=20\text{GHz}$ ,  $\epsilon_r=2.2$ ,  $h=5.2\text{mm}$ . All curves are normalized to the value derived for  $f_{\text{sc}}=20\text{GHz}$ ,  $\theta = 0$ .

Last but not least, an analytic expression of  $\alpha$  and  $\beta$  can be derived using the previous equations. Indeed, replacing  $P_{\text{ray}}^{\text{C}}(\theta, f)$  and  $P_{\text{T}[4]}$  in (22) by the obtained expressions from the ray optics approach [respectively (12) and (13)], it is possible to express  $\alpha$  and  $\beta$  in term of  $\theta, f, \epsilon_r, \bar{B}$ :

$$\alpha^2 + \beta^2 = \frac{2\varepsilon_r k_0^2 (f_{sc}) [1 - r(0, \varepsilon_r, f_{sc})]^2}{\pi [1 - r(0, \varepsilon_r, f_{sc})]^2} \times \left\{ 1 + \left[ \frac{4\bar{B}^2}{\varepsilon_r^{1/2} f_{sc}} (f_{sc} - f) \right]^{2.11} \right\}^{1/2} \quad (14)$$

The phase constant  $\beta$  depends on the scan angle  $\theta_p$  through the approximate formula [5]:

$$\beta = k_0 \sin(\theta_p) \quad (15)$$

It is seen that (15) remains very accurate when the scan angle is not too small [4] [the effect of the approximation is shown in Fig. 2a where  $\theta_p$  computed from (15) is given at three different frequencies]. The scan angle can be obtained from the ray optic approach:  $\theta_p$  is the angle for which the power pattern of the LWA (3) is maximum. It can be obtained 1) numerically from (3) [or (12) or (13)], or 2) by studding analytically (3) as done in section II (here a dielectric  $\varepsilon_r$  is taken into account). Thus, as previously derived, the solution of the following equation:

$$\varphi(\theta') = 2k_0 \sqrt{\varepsilon_r} h \cos(\theta') + (2N + 1)\pi, N = 0, 1, 2 \dots \quad (16)$$

gives  $\theta'_p$ , and the scan angle  $\theta_p$  is then obtained by (4). Note that as  $\varphi(\theta)$  can be expressed in terms of  $\theta, f, \varepsilon_r, \bar{B}$ , so  $\beta$  can also be expressed only with physical quantities coming from the ray optic approach. This expression of  $\beta$  can be used to obtain  $\alpha$  using (14), always with the same physical quantities. Fig. 8 shows a comparison of  $\alpha$  and  $\beta$  extracted from a TEN model and derived with ray optics formulas (14)-(16). The phase constant  $\beta$  computed numerically from (13) is also given. Note that both computations give exactly the same result as shown in Fig. 8. It is interesting to see that for a frequency lower than the splitting condition, that is to say when  $\beta$  is imposed to be null in first approximation, the value of  $\alpha$  computed by the ray optics approach is in good agreement with the one extracted from the TEN model. This approximation is thus relevant in such case, and this is true for all the configurations tested (two different configurations are shown in Fig. 8). At the splitting frequency and nearby surroundings, a significant error is observed because  $\beta$  is not actually equal to zero [5]. The condition  $\beta=\alpha$  in (14) has to be used, which rigorously corresponds to (11). For higher frequencies, in the neighborhood of the splitting frequency, the value of  $\alpha$  obtained with formulas (14)-(16) can still be used in first approximation with a good accuracy.

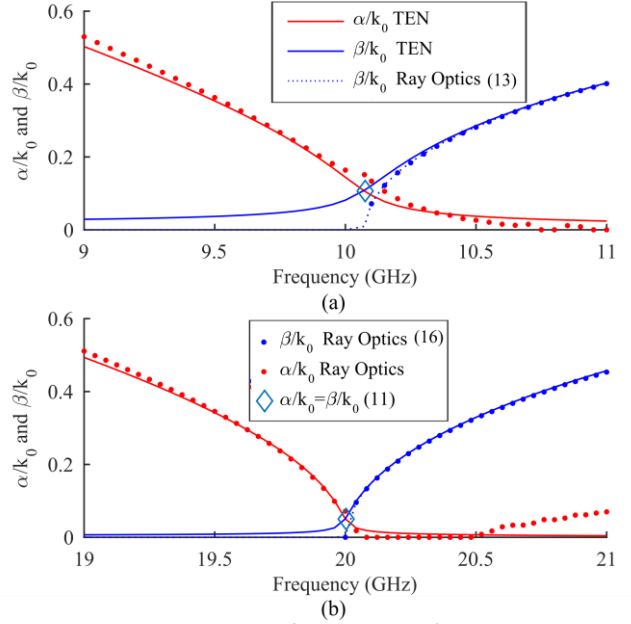


Fig. 8. Normalized attenuation  $\alpha/k_0$  and phase  $\beta/k_0$  constants of the TE LM versus the frequency extracted from a TEN model and derived with ray optics formulas (14)-(16), for two antenna configurations: a) the antenna parameters are given in Fig. 2:  $p=5\text{mm}$ ,  $L_s=4\text{mm}$ ,  $\varepsilon_r=1$ ,  $h=14\text{mm}$ ,  $f_{sc}=10\text{GHz}$ . b) The antenna parameters are given in Fig. 5:  $\bar{B}=20$ ,  $\varepsilon_r=2.2$ ,  $h=5.2\text{mm}$ ,  $f_{sc}=20\text{GHz}$ . Same legend for both plots.

#### IV. CONCLUSION

In this work, analytical formulas have been derived to analyze the splitting condition of Fabry Pérot Antennas (FPA) from a ray optics analysis approach. It has been shown that the classical formula used to compute the maximum power at boresight obtained from a ray analysis corresponds theoretically to the splitting condition that has been introduced from the leaky-wave approach. With the help of this formula, simple analytical expressions have been derived to aid in the design of these antennas, just as a function of the PRS reflectivity, frequency and the dielectric permittivity. An accurate formula describing the value of the leaky-mode phase and attenuation constants when the splitting condition is met have been obtained and an extended formula of the radiated power radiation, considering the presence of a dielectric substrate, have been also introduced. Thereby, this simple model does not require extracting the leaky mode propagation constants from a Transverse Equivalent Network (TEN) model

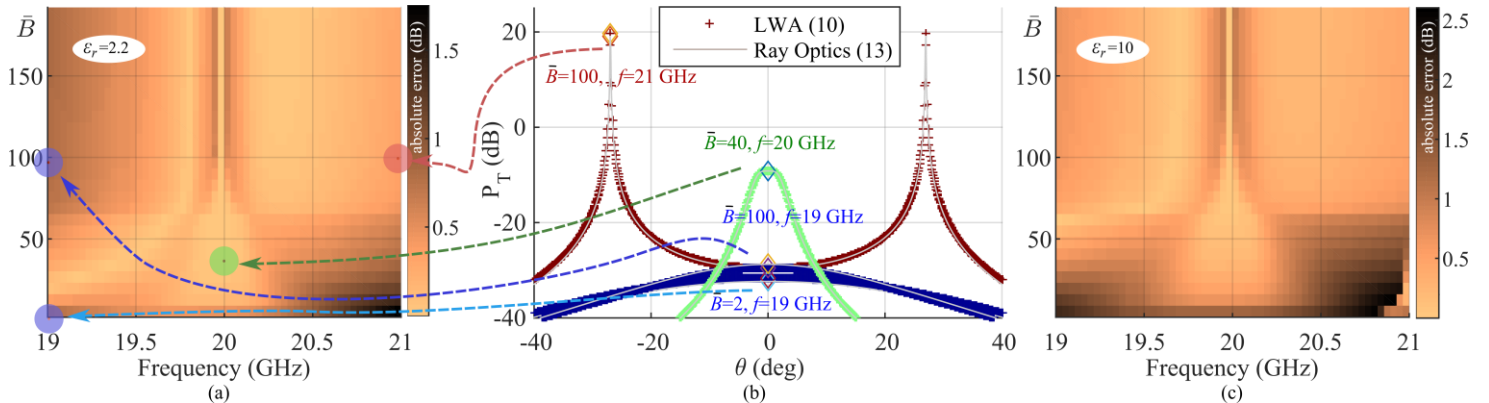


Fig. 7. Comparison study between (13) and (10) by varying  $\bar{B}$  and  $f$  on a wide range for the same antenna already used in Fig. 6. (a) Absolute error for  $\varepsilon_r=2.2$ . (b) Radiative power density computed with (13) and (10) as a function of  $\theta$  for 4 specific couples values of  $\bar{B}$  and  $f$ . (c) Absolute error for  $\varepsilon_r=10$ .

to compute the radiation pattern and the attenuation constant of this kind of leaky-wave antennas (LWAs).

#### APPENDIX I

The proof of (11) can be obtained by considering that (10) and (3) have to be equal up to a constant multiplier C:

$$C \cdot P_{T[4]} = P_T(\theta, f, \varepsilon_r) \quad (17)$$

Equation (11) gives an accurate value of  $\alpha$  and  $\beta$  when the splitting condition is met, that is to say, when  $\alpha=\beta$ , by considering (2) and when looking at broadside  $\theta = \theta' = 0$ . In such a case (17) can be rewritten as:

$$\alpha = \beta = \left( \frac{C [1 - r(0, \varepsilon_r)]^2}{2 [1 - r(0, \varepsilon_r)]^2} \right)^{1/2} \quad (18)$$

To obtain analytically the value of C, let us consider the condition  $\bar{B} \gg 1$  for which we should have [4, eq. 21], given below for simplicity (lossless configuration):

$$\alpha = \beta = \frac{\varepsilon_r^{3/4} k_0}{\sqrt{\pi \bar{B}}} \quad (19)$$

With (6), an approximation of  $r(0, \varepsilon_r)$  when  $\bar{B} \gg 1$  can be derived:

$$r(0, \varepsilon_r) = 1 - \frac{2\varepsilon_r^{1/2}}{\bar{B}^2} \quad (20)$$

By using (18) - (20), C can be extracted as follow,

$$C = \frac{2k_0^2 \varepsilon_r}{\pi} \quad (21)$$

and (11) is then directly deduced from (18) and (21).

#### APPENDIX II

The relation between [4, eq. (4)], [noted here (10) for  $P_{T[4]}$ ] and [2, eq. 13] (noted here  $P_{ray}^C$ ) is given by (22):

$$P_{T[4]} = (\alpha^2 + \beta^2) P_{ray}^C(\theta, f) \quad (22)$$

By considering (17), (21), (given in Appendix I) and (22), the relation between  $P_{ray}^C$  and  $P_T(\theta, f, \varepsilon_r)$  can be obtained in terms of  $\alpha$  and  $\beta$ . At the splitting condition,  $\alpha$  and  $\beta$  can be replaced using (11). Equation (12) is then obtained.

#### REFERENCES

- [1] G. V. Trentini, "Partially reflective sheet arrays," *IRE Trans. Antennas Propag.*, vol. 4, pp. 666–671, 1956.
- [2] R. Collin, "Analytical solution for a leaky-wave antenna," *IRE Trans. Antennas Propag.*, vol. 10, pp. 561-565, 1962.
- [3] A. P. Feresidis and J. C. Vardaxoglou, "High gain planar antenna using optimised partially reflective surfaces," *IEE Proceedings - Microwaves, Antennas and Propagation*, vol. 148, pp. 345-350, 2001.
- [4] G. Lovat, P. Burghignoli, and D. R. Jackson, "Fundamental properties and optimization of broadside radiation from uniform leaky-wave antennas," *IEEE Trans. Antennas Propag.*, vol. 54, pp. 1442-1452, 2006.
- [5] A. A. Oliner and D. R. Jackson, "Leaky-Wave Antennas," in *Chapter 11 of Antenna Engineering Handbook*, ed: J. L. Volakis, Editor, McGraw Hill, 2007.

- [6] C. Mateo-Segura, M. Garcia-Vigueras, G. Goussetis, A. P. Feresidis, and J. L. Gomez-Tornero, "A Simple Technique for the Dispersion Analysis of Fabry-Perot Cavity Leaky-Wave Antennas," *IEEE Trans. Antennas Propag.*, vol. 60, pp. 803-810, 2012.
- [7] J. L. Gomez-Tornero, F. D. Quesada-Pereira, and A. Alvarez-Melcon, "Analysis and design of periodic leaky-wave antennas for the millimeter waveband in hybrid waveguide-planar technology," *Trans. Antennas Propag.*, vol. 53, pp. 2834-2842, 2005.
- [8] D. R. Jackson, P. Burghignoli, G. Lovat, and F. Capolino, "The role of leaky waves in Fabry-Pérot resonant cavity antennas," *IEEE-APS Conf. Antennas Propag. in Wireless Communications (APWC)*, 2014, pp. 786-789.
- [9] Z. Tianxia, D. R. Jackson, J. T. Williams, and A. A. Oliner, "General formulas for 2-D leaky-wave antennas," *Trans. Antennas Propag.*, vol. 53, pp. 3525-3533, 2005.